

General Disclaimer

One or more of the Following Statements may affect this Document

- This document has been reproduced from the best copy furnished by the organizational source. It is being released in the interest of making available as much information as possible.
- This document may contain data, which exceeds the sheet parameters. It was furnished in this condition by the organizational source and is the best copy available.
- This document may contain tone-on-tone or color graphs, charts and/or pictures, which have been reproduced in black and white.
- This document is paginated as submitted by the original source.
- Portions of this document are not fully legible due to the historical nature of some of the material. However, it is the best reproduction available from the original submission.

Distribution Category UC-63
DOE/JPL-955201-79/3

LOW COST SOLAR ARRAY PROJECT:
Composition Measurements by Analytical Photon Catalysis

Third Quarterly Report

1 April 1979 - 30 June 1979

David G. Sutton, Luis Galvan, James Melzer and Raymond F. Heidner, III

The Ivan A. Getting Laboratories,
The Aerospace Corporation, El Segundo, California 90245



This work was performed for the Jet Propulsion Laboratory, California Institute of Technology, under NASA Contract NAS7-100 for the U.S. Department of Energy.

JPL Low-Cost Silicon Solar Array Project is funded by DOE and forms part of the Solar Photovoltaic Conversion Program to initiate a major effort toward the development of low-cost Solar Arrays.

(NASA-CR-158737) LOW COST SOLAR ARRAY
PROJECT: COMPOSITION MEASUREMENTS BY
ANALYTICAL PHOTON CATALYSIS Quarterly
Report (Aerospace Corp., El Segundo, Calif.)
22 p HC A02/MF A01

N79-26500

Unclas
CSCL 10A G3/44 27826

Technical Content Statement

This report contains information prepared by the Ivan A. Getting Laboratories of The Aerospace Corporation under JPL subcontract. Its content is not necessarily endorsed by the Jet Propulsion Laboratory, California Institute of Technology, National Aeronautics and Space Administration or the U.S. Department of Energy.

Table of Contents

	Page
I. Summary	4
II. Background	4
III. Progress During Reporting Period	5
IV. Ancillary Data	10
V. Conclusions	10
VI. Future Activity	11
VII. References	12
VIII. Figures	13

I. Summary

The object of this research is to assess the applicability of the photon catalysis technique for effecting composition analysis of silicon samples. In particular, our technique is to be evaluated as a detector for the impurities Al, Cr, Fe, Mn, Ti, V, Mo and Zr. During the first reporting period we have detected Al, Cr, Fe and Mn with the photon catalysis method. We have established the best fluorescence lines to monitor and determined initial sensitivities to each of these elements by atomic absorption calibration. In the course of these tests vapor pressure curves for these four pure substances have also been mapped.

During the second quarter we detected Ti and Si with our technique. The best lines to monitor were catalogued and vapor pressure curves were determined. Attempts to detect vanadium were unsuccessful due to the refractory nature of this element and the limited temperature range of our evaporator.

The third quarter was devoted to the study of impurities in silicon matrices. The evaporation process was shown to be congruent; thus, our spectral analysis of the vapor will yield the composition of the bulk sample. Qualitative analysis of metal impurities in silicon was demonstrated below the part per million level. Only one atomic spectral interference has been noted so far; however, it is imperative to maintain a leak tight system due to chemical and spectral interferences caused by the presence of even minute amounts of oxygen in the active nitrogen afterglow.

II. Background

Work commenced during the week of September 11 with the assembly of our Analytical Photon Catalysis (MTES)¹ device into a configuration suitable for the study of silicon impurities. The resulting instrument and its function can best be explained with reference to Figure 1. It consists of a vertical section of quartz tubing 9 cm in diameter. An electrically heated metal vapor furnace is attached to the bottom of the quartz tube, and a 60-1/sec pump, attached at the top of the quartz tube, provides the means to evacuate the system. Argon or Nitrogen injected through the bottom of the furnace assembly entrains the flow of metal atoms from the furnace and carries it into the quartz observation section. In this section, the concentration of Argon is much greater than the metal concentration. A thermocouple placed in contact with the metal in the furnace allows direct measurement of the metal atom source temperature, or an optical pyrometer may be employed by observing the heated metal down through the observation window.

A ring-shaped quartz gas injector is inserted into the apparatus at the junction of the furnace assembly and quartz flow tube. Through this injector, active nitrogen is introduced into the Ar-metal atom stream. The active nitrogen, consisting primarily of N atoms, $N_2(A^3\Sigma_u^+)$, and ground-state N_2 , was prepared upstream of the injector by passing N_2 gas through a 70-W microwave discharge.

The region of the quartz flow tube approximately 5 cm above the active nitrogen injector is monitored photoelectrically with an uncooled RCA 1P28 phototube attached to a one meter monochromator. Apart from neutral density filters, which are used at higher metal concentrations to avoid high photomultiplier tube current, no other optics are used. Hollow-cathode lamps can be placed on the opposite side of the flow tube and at the same height as the monochromator entrance slits. They are used as a line source for the atomic absorption measurements to calibrate the fluorescence intensity measurements with respect to metal vapor concentration.

The Ar and N₂ flows were adjusted to give a total pressure of 2-4 Torr. With the microwave generator set to deliver 70 W to the N₂ flow, a pale straw-colored glow is observable downstream of the injector. The furnace is then set to a given temperature, and the resulting atomic line emission intensities are measured.

The most intense and spectroscopically isolated lines are chosen (in accordance with Task 1A of the statement of work) to be the best fluorescence lines to monitor for the purposes of analysis. The intensity is a direct measure of the concentration of the emitting species and can be calibrated as specified in Task 1B at high source temperatures by the atomic absorption technique. If one plots the $\log I$ vs $10^4/T(K)$ a vapor pressure curve results as per Task 1C. These three tasks applied to Al and Cr Fe and Mn have occupied us for the first quarter. During the second quarter we completed Tasks IABC by our examination of titanium, vanadium and silicon.

The third quarter was scheduled for examination of the NBS standard silicon (SRM57), the identification of chemical and spectral interferences and to determine the extent of selective evaporation of impurities (Tasks IDEF respectively). We have effectively completed these tasks. In addition, two other silicon samples have been investigated. (SPEX Industries 5-9's and 6-9's material).

III. Progress During Reporting Period

Most of our time during April was devoted to the continued analysis of NBS Si (SRM57). In the second quarterly report we gave the results of our preliminary qualitative analysis of this material. The table of identified lines is reproduced here.

Element	Wavelength of Prominent Lines Observed from SRM57, nm
Si	251.6, 288.2
Al	308.2, 309.2
Cr	359.4, 425.4
Mn	279.5, 403.1
Fe	239.5 (?)
Mg	285.2

Cu	324.7, 515.3
Na	330.2 (background impurity)
Ca	422.7, 487.8

We also discussed the mathematics of congruent evaporation. In so doing we showed that the vapor pressure curves obtained by following the fluorescence of the impurities should have the same slope as that obtained from the fluorescence of the host. Figure 15 of the second quarterly clearly shows this trend for the Ca and Al impurities in SRM57. During April we extended these measurements by following the intensities of additional lines due to impurities as a function of the source temperature. These measurements included the Al (309.2), Ca (422.7), Cr(359.3), Cu(324.7), Mn(403.4) and Si(251.6) lines. The resulting curves were all well represented by straight lines. The slopes of each line was determined by least squares fitting and compared to the slope obtained from the silicon 251.6 line. This comparison and the comparison of the slope obtained from the vapor pressure curve measured over the pure material is compared in Figure 16. In this figure the relative slopes obtained from measurements over the pure material are plotted as circles and the vapor pressure data obtained from Si (SRM57) is plotted as squares.

It is immediately evident from the figure that the vaporization rate (as manifested by the slope of the apparent vapor pressure curves) of each of the impurities tends toward the host material. This is particularly evident in the case of calcium where the change in slope is more than a factor of three. This figure constitutes powerful evidence that the vaporization process is congruent, and that fractional distillation or segregation and independent evaporation is not the dominant mechanism of the evaporation process. This evidence becomes particularly convincing when we point out the range of melting points (Mg 650°C-Cr 1875°C) and the range of concentrations (Mg .01% - Al .67%) encompassed by the five impurities studied. Thus we conclude that our analysis of the vapor will be equivalent to a bulk analysis of the solid sample.

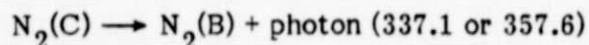
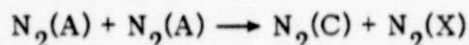
Interferences encountered so far have mainly been of a spectral nature. The only chemical effect noticed was produced inadvertently. When pure manganese was being studied the crucible was overheated causing the deposition of manganese on our nitrogen injector and on walls of our quartz observation tube. We immediately noticed a drop in the intensity of the normal afterglow and a heating of the walls as well as loss of fluorescence signal.

The explanation is simple. Manganese promotes the heterogeneous recombination of nitrogen atoms. This occurs on the surfaces coated with manganese. The active nitrogen (normally produced by homogeneous, gas phase recombination of nitrogen atoms) is thereby quenched. The heat liberated by the heterogeneous process is absorbed locally on the wall. Careful cleaning eliminated the problem and restored the usual Lewis-Rayleigh afterglow and the MTES signal.

It is extremely unlikely that enough metal would be plated out under normal operating conditions to seriously affect the system performance. In addition, not all metals are as efficient as Mn in catalysing heterogeneous N atom recombination. However, after long hours of service at high temperature system performance may drop off. Simple cleaning will rectify the situation and this caveat should serve to alert potential users.

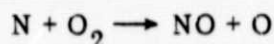
Spectral interferences are minimal in a leak tight system. The only overlap of atomic lines observed so far is between Na and Mg at 285.2 nm. Na is present as background. Baking out the crucible and insulation eliminates the sodium lines. In addition, there are usually ancillary lines available for each element if an unlikely overlap is encountered. Some of these lines were cataloged in the second quarterly report.

More serious in nature are the molecular bands due to N_2 and if leaks are present NO and N_2 . There will always be small signals due to the N_2 second positive emission. A sample background spectrum was shown in Figure 13 of the second quarterly report. This was taken with an empty berlium oxide crucible heated to 1500°C. The Na feature in that figure at 330.2 nm will diminish with time. The band at 337.1 nm is excited by energy pooling between two excited metastable $N_2(A)$ molecules to form one $N_2(C)$ and a ground state molecule. The $N_2(C)$ species then radiates at 337.1 nm and to a lesser extent at 357.6 nm. The pooling reaction and subsequent emission mechanism has been studied by Setser and can be represented as follows:



Since $N_2(A)$ is responsible for our MTES signal as well, there is nothing we can do to eliminate this possible interference. Fortunately, however, the intensity from this transition is low and the bands are narrow.

Much more serious interferences are caused by leaks. NO is produced by the reaction



and is excited by collisions with $N_2(A)$ molecules. The resultant emission from NO is normally confined to the gamma bands shown in Figure 17. Sometimes with large leaks the beta bands are also observed. See Figure 18. Worse still NO is known to catalyze the pink afterglow of nitrogen. The spectral signature of this glow is shown in Figure 19. The dominant emission is from the N_2 first negative systems. Unfortunately all of these emissions involve extensive, intense band systems in the useful spectral region for atomic emission spectrometry (200-500 nm). Fortunately the cure for this malady is simple. Fix the leaks.

May was devoted to the study of higher purity silicon. In particular, we examined SPEX Industries 5-9's grade. This powdered material is advertised to be greater than 99.999% pure. The sample we obtained was identified as lot number 12771. The following semiquantitative analysis was supplied with the material (See Figure 20).

Element	ppm
Cu	4-8
Al, Fe	0.5-2.0
Mg	0.1-0.5

Spex Industries representatives have explained to me that this analysis is obtained by spark photometry.

Our goals in examining this material are twofold. First we want to verify qualitatively that our analysis method is sensitive to metal impurities in a silicon matrix at the ppm level. Second, congruent evaporation needs to be demonstrated with high purity material in addition to the tests run with Si (NBS-SRM57) of 97% purity.

The results of the semiquantitative analysis were spectacular. The spectrum shown in Figure 20 displays most of the major spectral features used in our analysis. It was obtained when a sample of Spex 5-9's silicon was placed in one of our boron nitride crucibles, heated to 1500°C and the resulting vapor mixed with active nitrogen. The presence of all the elements, except Fe, identified as impurities by SPEX can be verified by two or more atomic emission lines. In addition, we can positively identify Cr and Ga by their emission signatures. These last two elements were not detected by SPEX's analysis technique.

The Na emission line at 330.2 nm is due to the background presence of this element in the crucible or the insulating material. The 330.2 nm line is present in the blank spectrum when we heat an empty crucible. See Figure 13 of the Second Quarterly Report (Jan.-March 1979). Unlike any of the other atomic lines shown in Figure 20, it slowly diminishes in intensity during the course of an experiment. We can therefore conclude that Na is not an integral impurity of the SPEX 5-9's silicon and that it is slowly being eliminated from the high temperature section of our apparatus. In contrast, none of the other atomic line intensities change in intensity due to time alone. This fact is further evidence that the evaporation process is congruent. If selective evaporation were taking place, the composition of the sample would be constantly changing. This would manifest itself in time varying intensities for all or most of the impurity lines. Thus our failure to observe any time variations in the intensity of the impurity emission lines is further proof of our contention that the composition of the vapor is representative of the original sample.

Further proof of this hypothesis is contained in Figure 21. It compares the slopes of the vapor pressure curves obtained from the atomic emissions due to impurities to the slope of the VP curve obtained from the silicon line at 251.6 nm.

In the Second Quarterly Report (Jan - March 79) we showed mathematically that congruent evaporation would lead to parallel VP curves. Ideally this would manifest itself in a plot like Figure 21 where each point had an ordinate equal to one. In the April monthly report we included a plot, Figure 16, summarizing our VP slopes obtained with Si from NBS-SRM57. That Figure clearly showed the trend toward parallel VP curves. Figure 21 is an identical plot, but derives from data taken on SPEX 5-9's silicon.

The two Figures, 16 and 21, are almost identical. They both clearly show the trend toward parallel slopes; i.e., the approach toward congruent evaporation.

In June we obtained the MTES qualitative analysis of SPEX 6-9's silicon. This material is advertised to have less than one part per million total impurities. In fact their spectrographic analysis is incapable of detecting any impurities. In contrast we show in Figure 22 the MTES spectrum obtained with this material and a background spectrum taken with an empty crucible.

The background spectrum was recorded with one hundred times more sensitivity than the silicon spectrum. The only element that appears in the background is sodium. The intensity of these lines at 330.2 nm and 285.3 nm diminish slowly on bake-out. Thus, the 330.2 nm line does not appear in the silicon spectrum, since it was baked-out prior to adding the Spex 69's sample to the crucible. The Na line at 285.3 interferes with the 285.2 nm Mg line. We have noted only this one atomic interference to date.

The impurities Mg and Ca are clearly in evidence in our sample spectrum. Thus, if Spex's analysis is correct we have demonstrated sensitivity at less than one part per million. Interestingly, the ion lines from both these group IIA impurities have higher intensities than the neutral lines. Compare 279.6 nm with 285.2, for example. The Ca neutral line at 422.7 is weak and is not shown in the figure. This result belies our previous explanations of the excitation mechanism. We hypothesized that bimolecular collisions with $N_2(A^3\Sigma)$ was the source of excitation of the neutral atomic emission lines. Obviously this one step mechanism can not explain the excitation of ionic states at 9 to 12 eV (roughly twice the A state term value).

Nevertheless, we decided to empirically determine if the ion lines of Ca would be useful in an analysis of Si samples. Thus we determined the intensity of the 393.4 nm Ca II as a function of source temperature to see if the vapor pressure plot paralleled that of the silicon host. The results are shown in Figure 23. It is evident that the calcium ion line tracks the silicon intensities even more faithfully than the neutral Ca 422.7 nm line. We thus conclude that this line in particular will be useful for analysis.

IV. Ancillary Data

The gallium impurity in the SPEX 5-9's material was easily identified with reference to our earlier work (Aerospace Sponsored Research) on the detection of gaseous metal compounds. In particular, the same four gallium lines identified in Figure 20 were observed when triethyl gallium was mixed with active nitrogen. In addition, we have observed that active nitrogen excites identical spectra from trimethyl bismuth and pure bismuth vapor. The same can be said for SiH_4 and silicon metal vapor. Thus, for the purposes of aiding potential users in identifying a wide variety of impurities we include here an auxiliary list of MTES lines. Most were obtained using metal alkyls and hydrides as sources. The ramifications of this earlier work with gaseous compounds might eventually lead to MTES analysis and monitoring of gaseous feedstocks and doping material used in the manufacture of solar grade silicon and in the fabrication of cells.

element	best MTES lines (nm)	ancillary lines nm
As	228.8, 235.0	193.7, 197.0
Bi	306.8	223.0, 289.8
Ga	403.3, 417.2	287.4, 294.3
Ge	265.1, 303.9	270.9, 275.4
Mg	285.2	279.1(II), 279.8(II)
P*	251.8	246.6, 260.5

*The wavelengths given for phosphorous are actually the band heads for the PN ($A^1\Pi - X^1\Sigma$) transition.

V. Conclusions

Analysis of the vapor pressure curves of the impurities in NBS silicon (SRM57) indicates that the vaporization is congruent. Successful qualitative analysis of the SPEX 5-9's material clearly demonstrates the sensitivity of our MTES technique to silicon impurities at the ppm level. Our detection of gallium and chromium shows that we have more sensitivity than the spark photometry method employed by SPEX. The high signal to noise level evident from Figure 20 portends well for our quest to achieve 10 ppb sensitivity.

The parallel vapor pressure curves and time independent intensity relations are antithetical to the occurrence of selective evaporation (fractional distillation of impurities). We conclude that the composition of the bulk solid can be determined by evaporation and subsequent analysis of the vapor.

The detection of Mg and Ca in the Spex 6-9's material indicates that MTES is sensitive to impurities present at less than a part per million. The Ca ion lines are more persistent than the MTES emission from the neutral atom and is useful for analysis by this technique.

Chemical interferences have not been encountered under normal operating conditions. Atomic spectral interferences are not frequently encountered and can be circumvented easily. N_2 second positive bands may cause spectral interferences occasionally. Atmospheric leaks must be scrupulously avoided in order to eliminate the extensive spectral interferences of the NO beta and gamma systems and the pink nitrogen afterglow.

VI. Future Activity

The Spex Si samples and various samples available through the Jet Propulsion Laboratory will be analyzed. Our goals will be to demonstrate sensitivity to impurities at concentrations below 100 parts per billion, to establish a general set of advantageous running conditions and to construct analytical curves for several impurities. The dynamic range of the MTES technique will be tested by analyzing samples that contain a common impurity in a wide range of concentrations.

VII. References

1. The term Metastable Transfer Emission Spectrometry, MTES, is somewhat more descriptive and is used synonymously with Analytical Photon Catalysis. See Rev. Sci. Instrum. 49, 1124 (1978).
2. Ralph Hultgren, et al., "Selected Values of Thermodynamic Properties of Metals and Alloys," John Wiley and Sons, Inc. (New York - 1963).
3. An. N. Nesmeyanov, "Vapor Pressures of The Elements," translated and edited by J.I. Carasso (Academic, New York, 1963).
4. C.H. Corliss and W.R. Bozman, "Experimental Transition Probabilities for Spectral Lines of Seventy Elements," (NBS Monograph 53, 1962).
5. M. Pinta, "Detection and Determination of Trace Elements," Ann Arbor Science Publishers, Inc. (Ann Arbor, Mich., 1962).
6. S. Dushman, "Scientific Foundations of Vacuum Technique," edited by J.M. Lafferty, John Wiley and Sons, Inc. (New York, 1962).
7. D.H. Stedman and D.W. Setser, J. Chem. Phys. 50, 2256 (1969).
8. G.E. Beale, Jr. and H.P. Broida, J. Chem. Phys. 31, 1020 (1959).
9. D.G. Sutton, J.E. Melzer, and G.A. Capelle, Analytical Chem. 50, 1247 (1978).

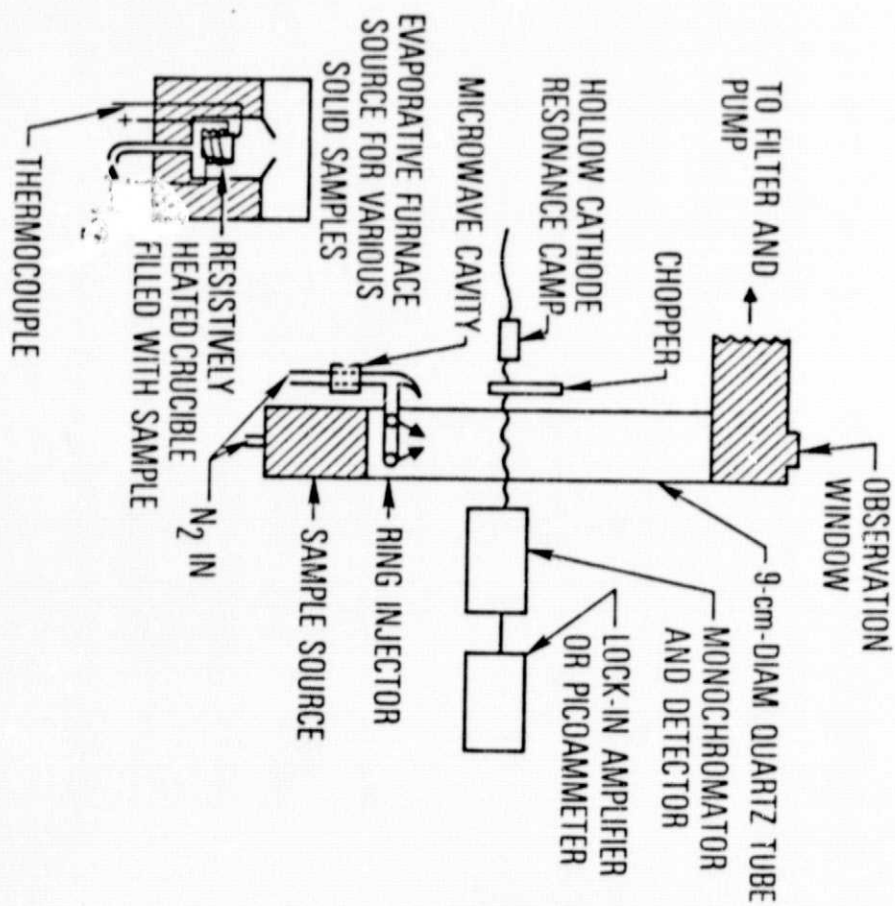


Figure 1: Schematic for MTES Apparatus

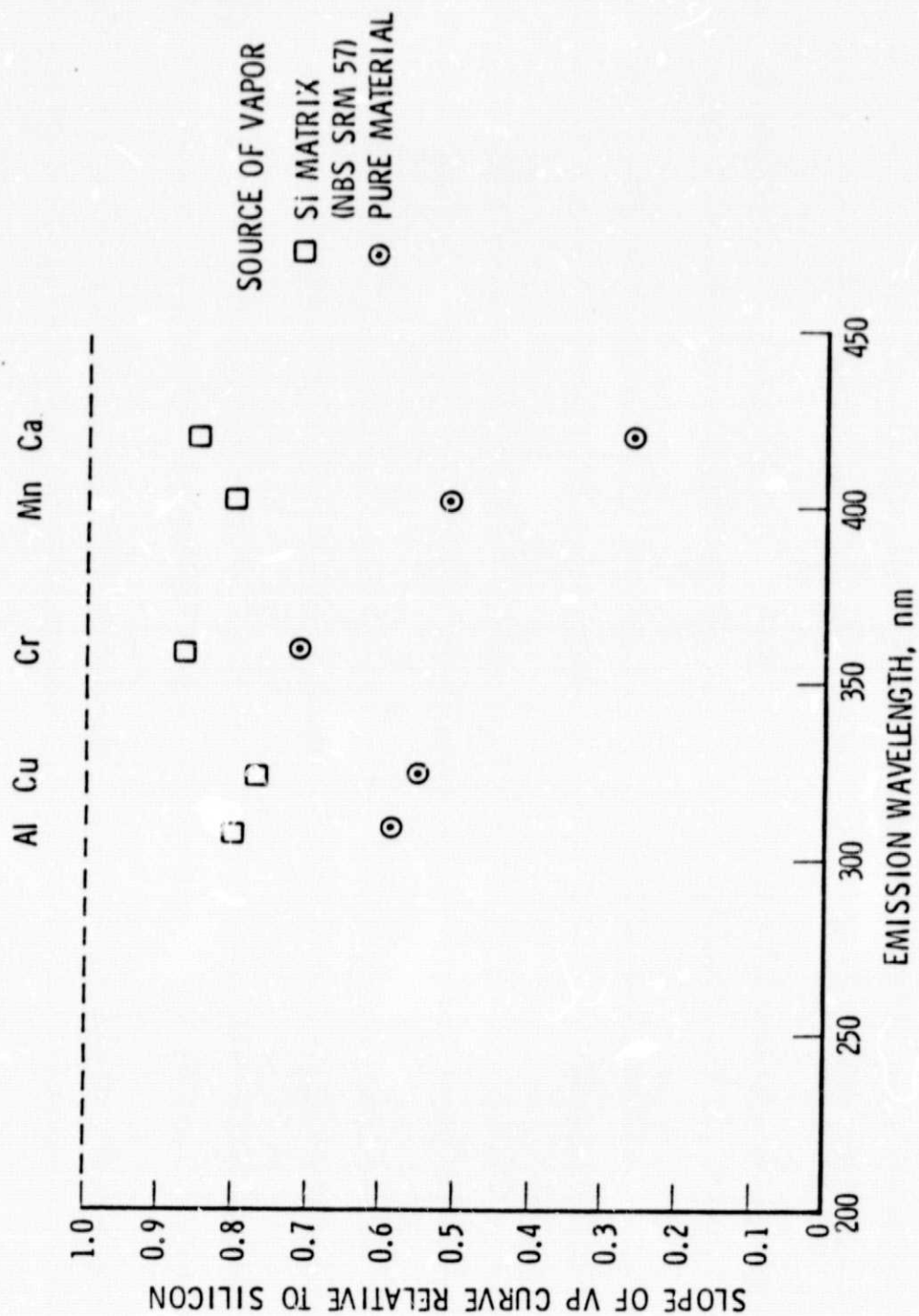


Figure 16: Evidence for Congruent Evaporation of Si SRM 57

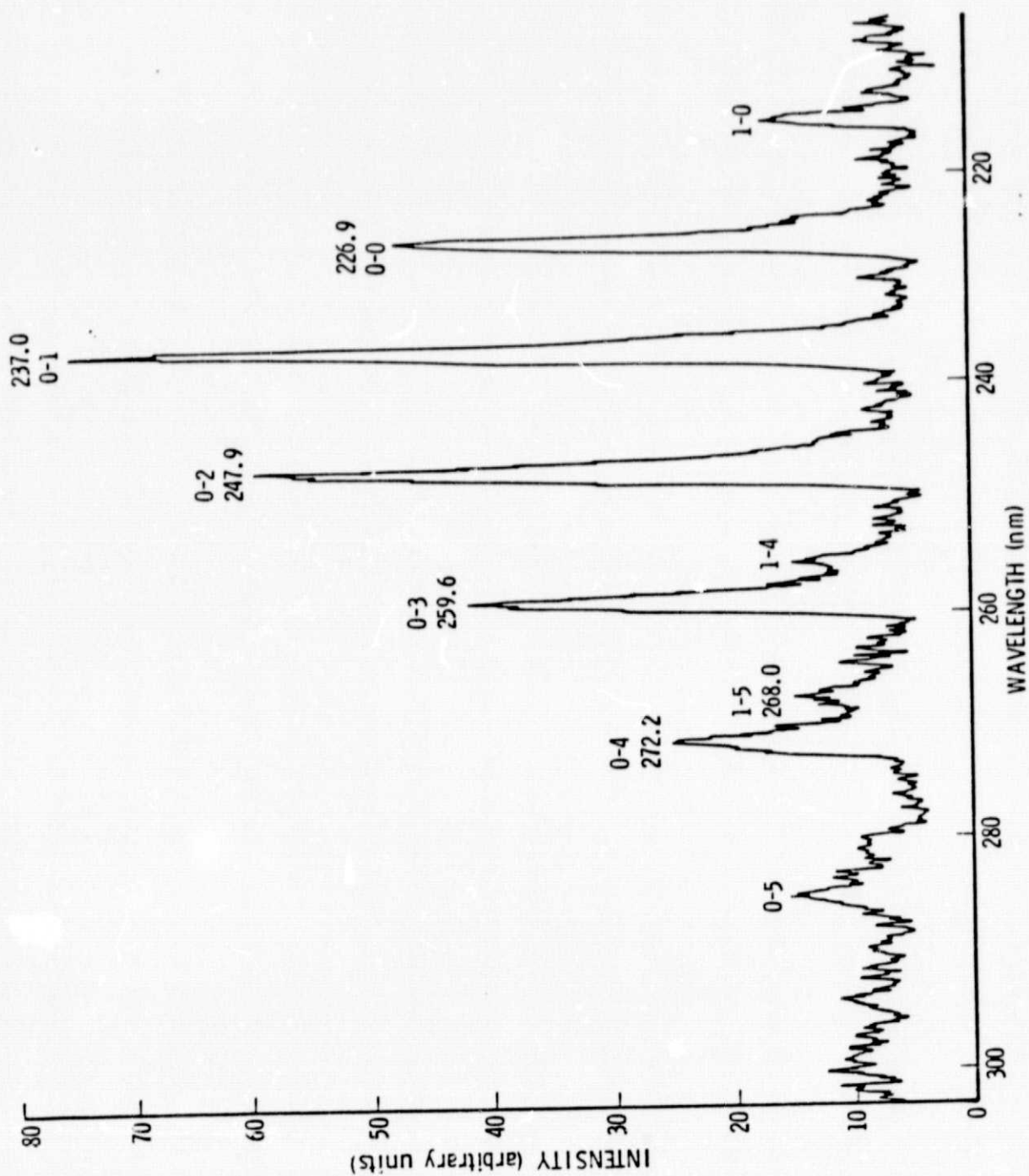


Figure 17: NO Gamma Bands Excited by Active Nitrogen

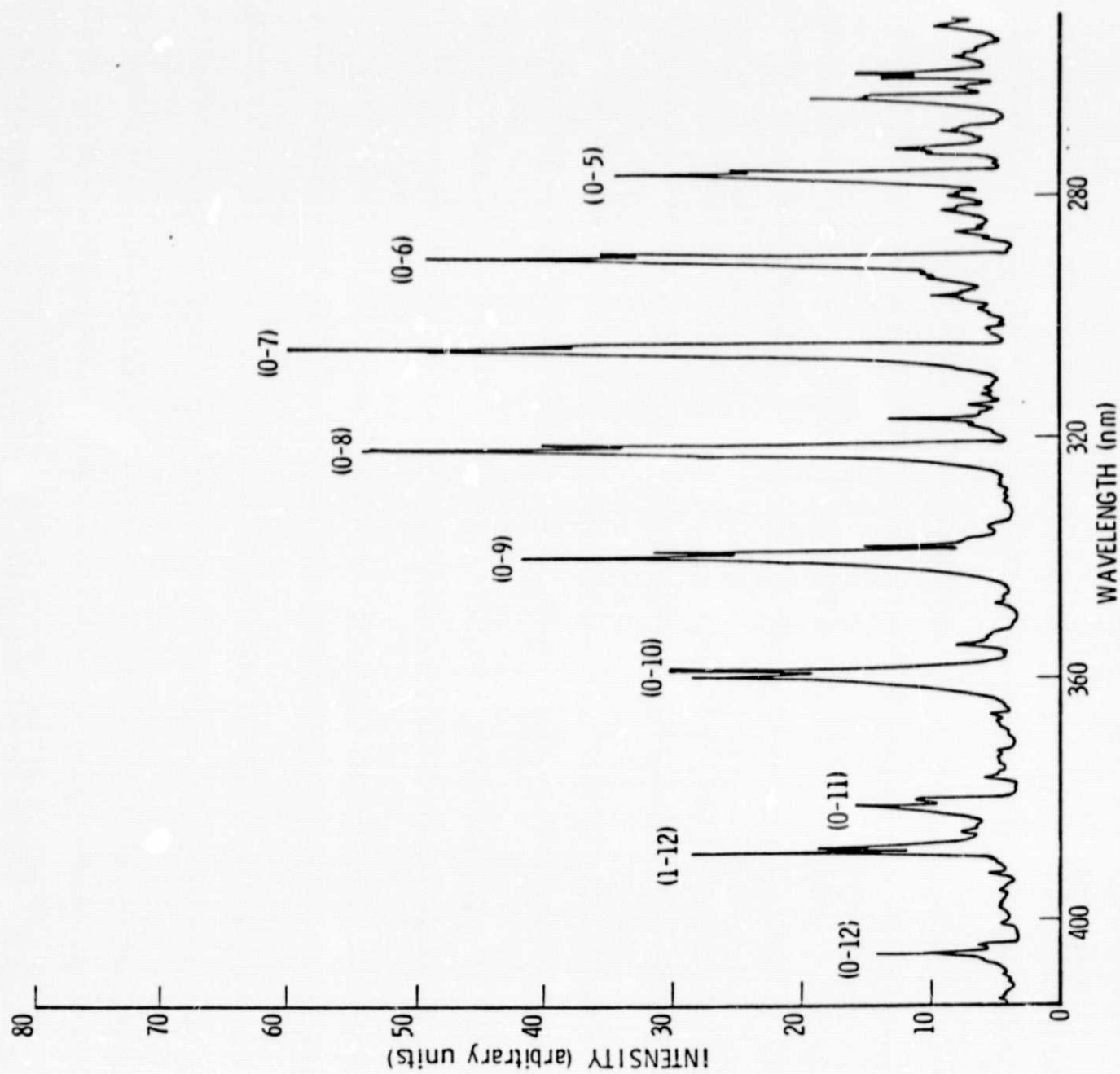


Figure 18: NO Beta Bands Excited by Active Nitrogen

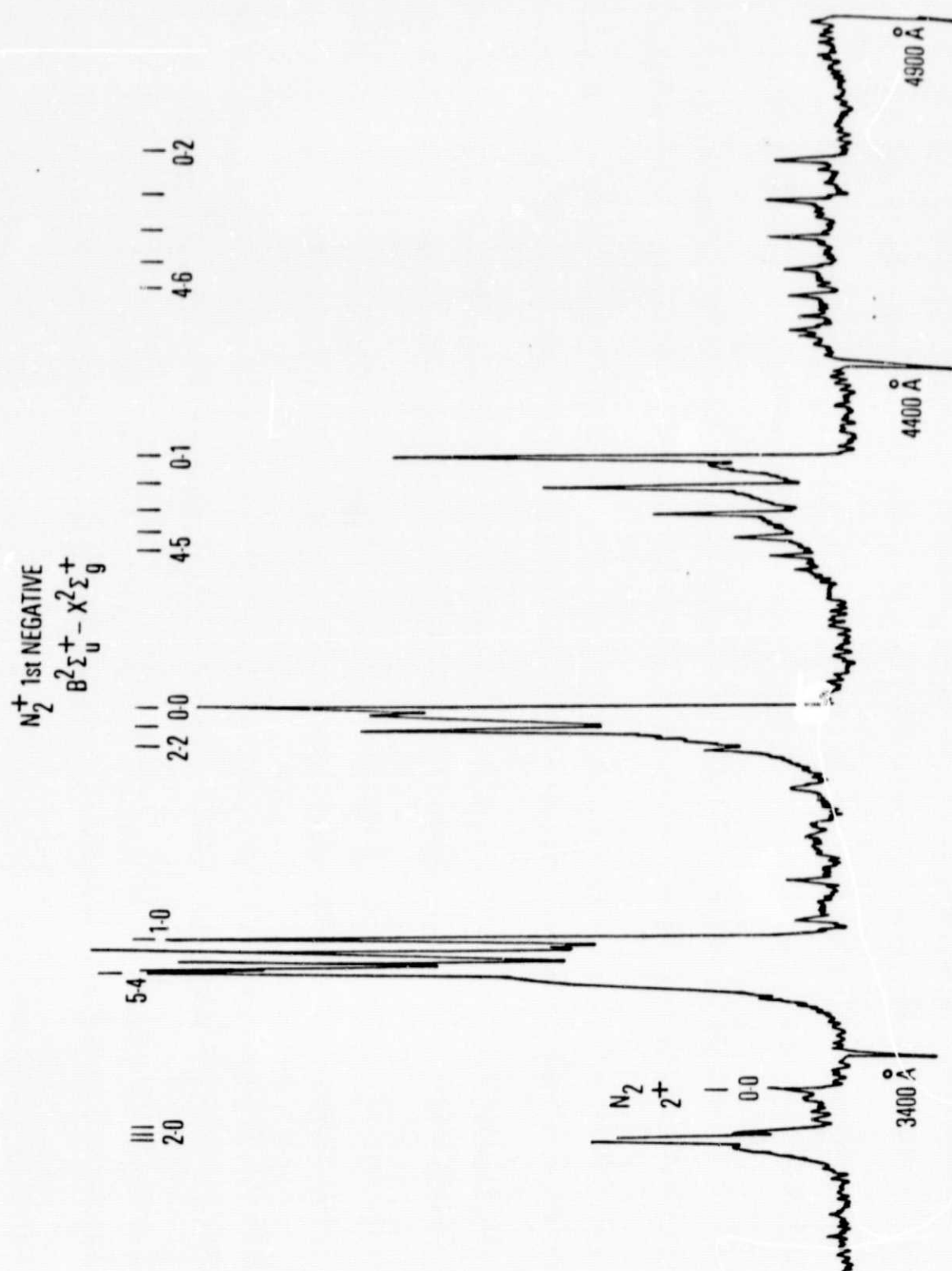


Figure 19: Spectrum of Pink Afterglow in Active Nitrogen

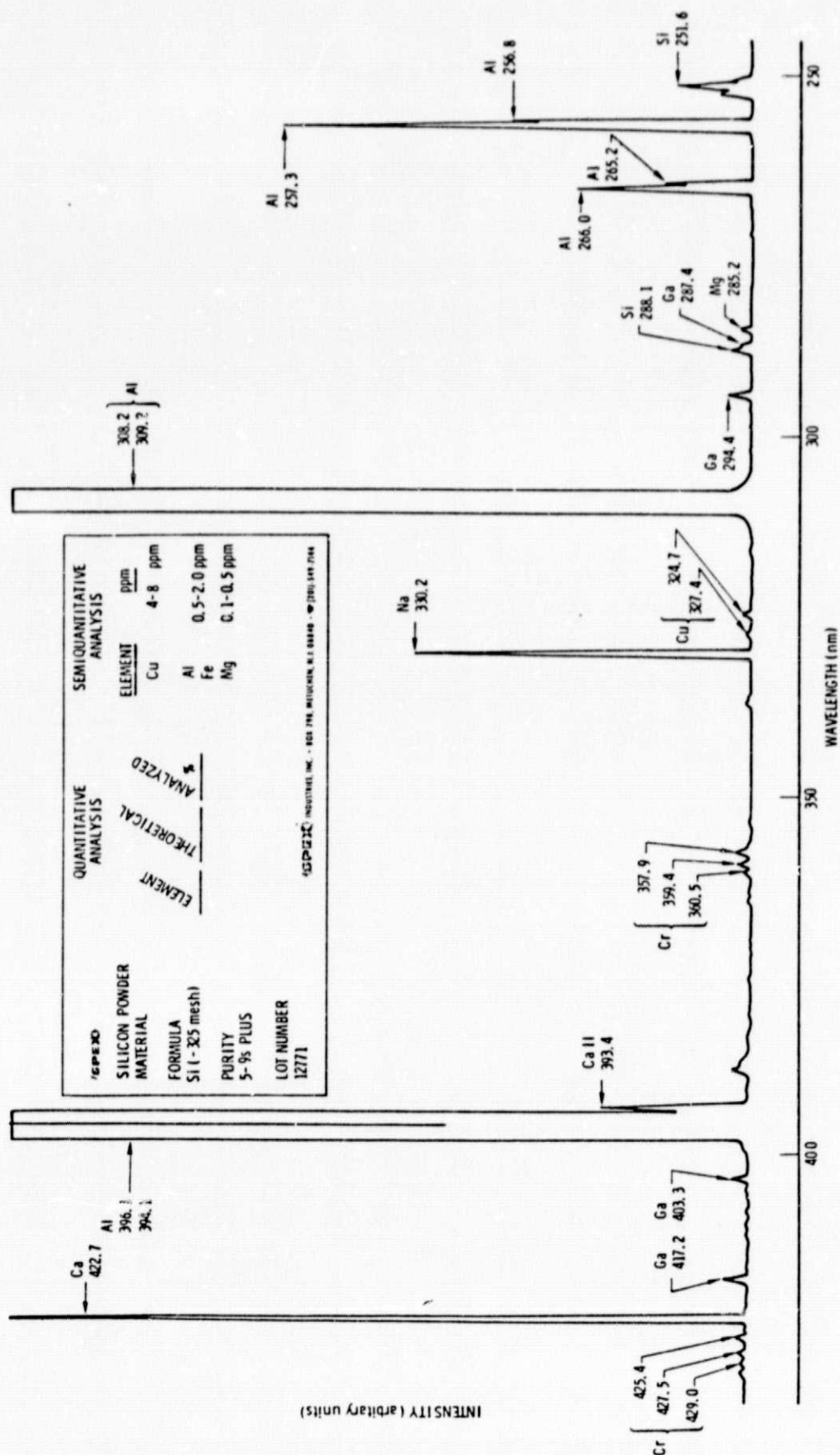


Figure 20: MTES Spectrum for Si (SPEX 5-9's)

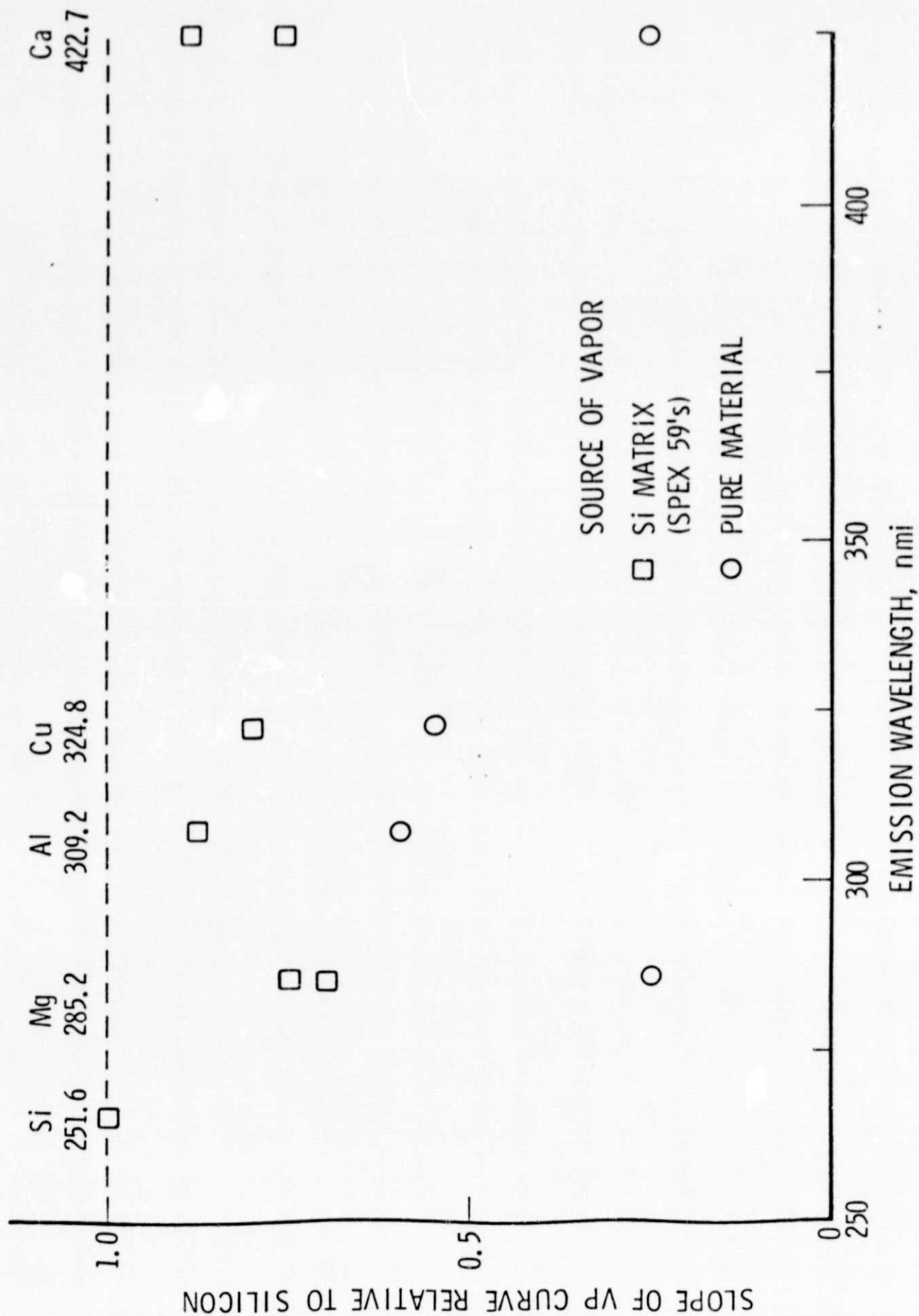


Figure 21: Evidence for Congruent Evaporation of Si (SPEX 5-9's)

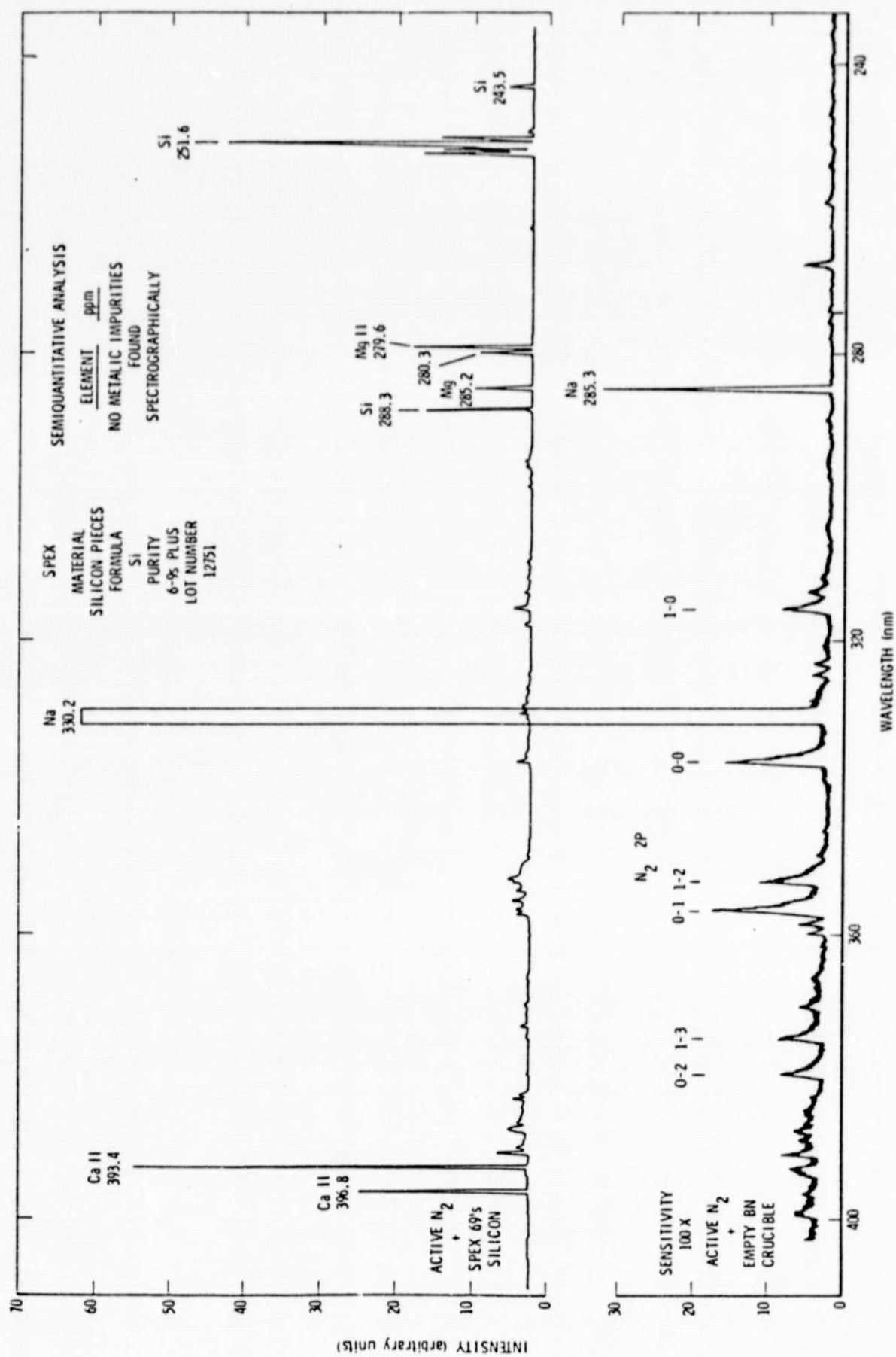


Figure 22: MIES Spectrum for Si (CPEX 6-9's)

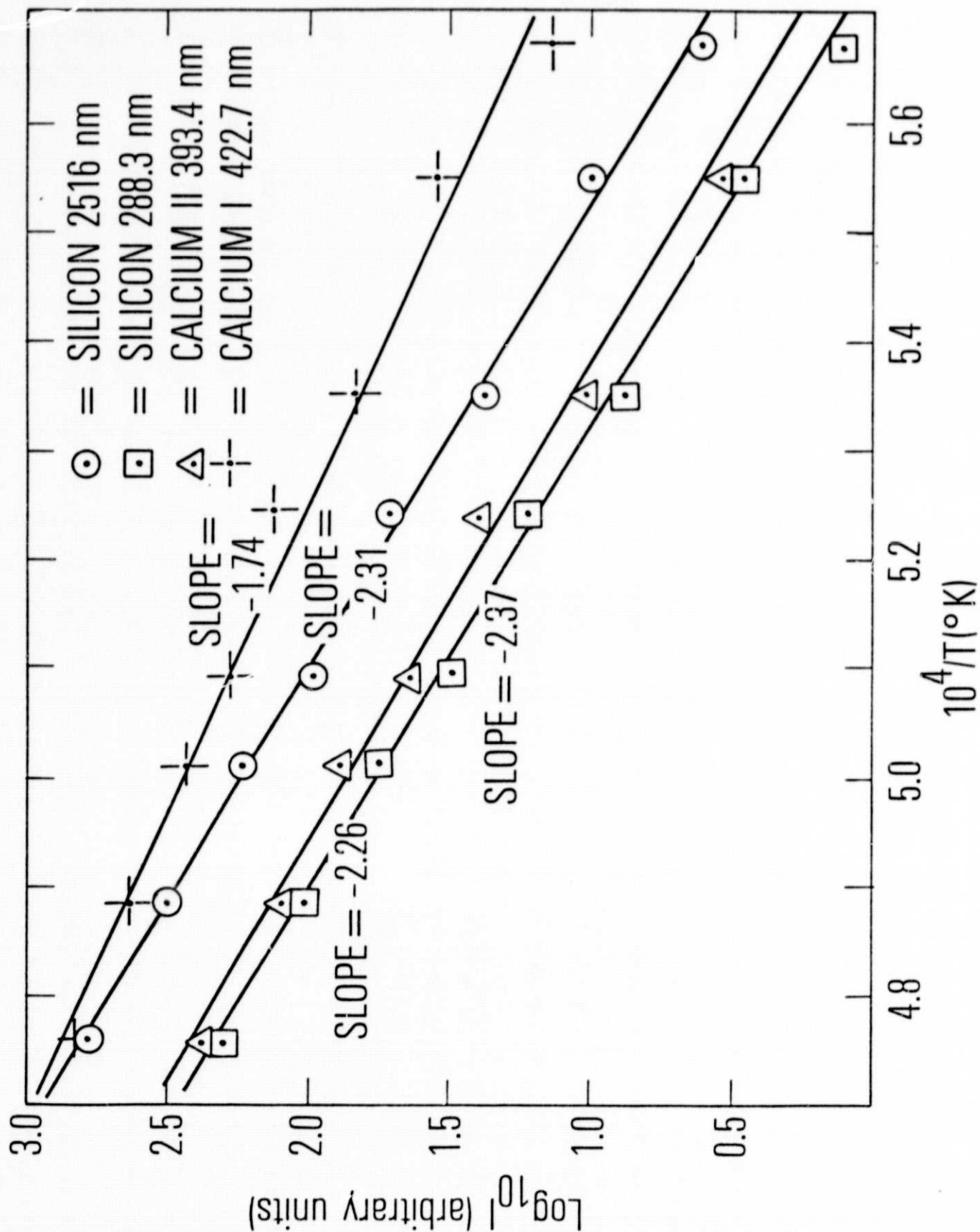


Figure 23: MIES Vapor Pressure Curves for Si (SPEX 6-9's)